THE ASTROPHYSICAL JOURNAL, 446:598–601, 1995 June 20

THE EXTREME ULTRAVIOLET SPECTRUM OF THE BL LACERTAE OBJECT PKS 2155−304

ARIEH KÖNIGL,[1] JOHN F. KARTJE,[1] STUART BOWYER,[2] STEVEN M. KAHN,[3] AND CHORNG-YUAN HWANG[2]

Received 1994 October 24; accepted 1994 December 22

ABSTRACT

We carried out two spectroscopic observations of the BL Lacertae object PKS 2155−304 with the *Extreme Ultraviolet Explorer* during 1993 June (∼111 ks) and July (∼157 ks). The source was detected in the ∼75–110 Å range during both epochs, but the two spectra differ in detail, and the flux has increased by ∼60% between the two observations. A power-law fit to the data yields an energy spectral index $\alpha \approx 3$–4 for the measured Galactic H I column density and likely choices of the He I and He II abundances: such values are inconsistent with the soft X-ray spectral index of 1.65 measured by the *ROSAT* Position Sensitive Proportional Counter, which approximately corresponds also to the observed flux ratio of EUV to X-ray. Fitting a power law with $\alpha = 1.65$ to the EUV data implies strong absorption at the source between ∼75 and ∼85 Å. We argue that this absorption is not due to continuum opacity and demonstrate that it can be attributed, instead, to a superposition of Doppler-smeared absorption lines originating in high-velocity ($\lesssim 0.1c$), radially localized, broad emission line–type clouds of total column density $\sim 5 \times 10^{20}$ cm^{-2} that are ionized by the beamed continuum of the associated relativistic jet. We identify the lines as mostly L- and M-shell transitions of Mg, Ne, and Fe. The same model also implies a pronounced O VII Kα X-ray absorption feature at roughly the same energy as the feature detected in 1990 by BBXRT, which provides strong support for the apparent association of this object with a galaxy at $z = 0.116$. We suggest that the higher energy X-ray absorption feature detected in 1980 by the *Einstein* Objective Grating Spectrometer and identified with a broadened O VIII Lyα line might have originated in outflowing clouds that had a higher abundance of O VIII than of O VII, possibly because they crossed our line of sight closer to the continuum source.

Subject headings: BL Lacertae objects: individual (PKS 2155−304) — galaxies: jets — ultraviolet: galaxies — X-rays: galaxies

1. INTRODUCTION

BL Lacertae objects (BLOs) are highly variable active galactic nuclei that are characterized by a featureless continuum extending from radio to X-ray wavelengths (e.g., Maraschi, Maccacaro, & Ulrich 1989). They have been interpreted as relativistic jets whose beamed synchrotron and inverse-Compton emission dominates the measured spectrum because they are observed at small angles to the jet axis (Blandford & Rees 1978). They often appear in association with low-redshift ($z \lesssim 0.1$) elliptical galaxies, but it has been suggested that at least some of these objects correspond to gravitationally lensed quasars located at higher redshifts (e.g., Ostriker & Vietri 1990). PKS 2155−304 is one of the brightest extragalactic sources at all wavelengths and is considered to be representative of X-ray–selected BLOs. It has been the subject of several monitoring campaigns, including one recently with the *IUE* (Urry et al. 1993) and *ROSAT* (Brinkmann et al. 1994), which established the presence of correlated, $\gtrsim 20\%$ X-ray and UV intensity variations on timescales of hours.

One of the most puzzling aspects of X-ray–selected BLOs is the nature of the $\gtrsim 0.5$ keV X-ray absorption feature indicated in several of these objects (Madejski et al. 1991). Such a feature was first detected in *Einstein* Objective Grating Spectrometer (OGS) observations of PKS 2155−304 in 1980 May, which revealed an edge or a trough starting at 0.6 keV and extending to higher energies by 50–100 eV (Canizares & Kruper 1984). This feature has been interpreted as an O VIII Lyα line originating in a mildly relativistic ($\sim 0.1c$) outflow at the redshift ($z = 0.116$; Falomo, Pesce, & Treves 1993) of the apparent host galaxy (Krolik et al. 1985). BBXRT observations in 1990 December (Madejski et al. 1994) have confirmed the existence of a pronounced absorption feature but found that it started at an energy (∼510 eV) that was formally inconsistent with the OGS measurement a decade earlier. Furthermore, the feature appears to have weakened between the two observations, a result indicated also by *ROSAT* Position Sensitive Proportional Counter (PSPC) measurements in 1991 November (Brinkmann et al. 1994).

PKS 2155−304 was also found to be the brightest extragalactic EUV source in the all-sky surveys conducted by the *ROSAT* Wide Field Camera (WFC) (Pounds et al. 1993) and the *EUVE* (Bowyer et al. 1994). In each of these surveys, the detection was significant only in the shortest wavelength bandpass. *EUVE* observations carried out over ∼30 ks in 1992 July as part of the deep survey (Marshall, Carone, & Fruscione 1993) and the in-orbit spectrometer calibration (Fruscione et al. 1994) have revealed that the source is variable (at the ∼10% level) on a timescale of hours but that its flux level and spectral shape in the ∼75–110 Å wavelength range are compatible with an extrapolation of the power-law soft X-ray (∼0.2–2 keV) spectrum (of energy spectral index $\alpha \approx 1.65$) measured by the *ROSAT* PSPC. Given the various observational uncertainties, this value of α is also compatible with the EUV measurements by the *ROSAT* WFC (Brinkmann et al. 1994), and it thus appears that any break to the flatter ($\alpha < 1$) spectrum recorded by the *IUE* (Urry et al. 1993) does not occur at wavelengths shorter than ∼124 Å.

[1] Department of Astronomy and Astrophysics and Enrico Fermi Institute, University of Chicago, 5640 South Ellis Avenue, Chicago, IL 60637.
[2] Center for EUV Astrophysics and Astronomy Department, University of California, Berkeley, Berkeley, CA 94720.
[3] Departments of Physics and Astronomy, and Space Sciences Laboratory, University of California, Berkeley, Berkeley, CA 94720.

These observations are consistent with the entire UV–soft X-ray spectrum in PKS 2155−304 originating in a synchrotron emission component from a relativistic jet.

In this paper we report on two *EUVE* spectroscopic observations of PKS 2155−304 that have enabled us, for the first time, to conduct a detailed EUV spectral analysis of an extragalactic object. Our observations have provided valuable clues to the redshift of this BLO, the interpretation of its enigmatic X-ray absorption feature, and the presence of broad emission line region (BELR) gas in its nucleus. These results are particularly significant in view of the fact that the beamed nonthermal continuum in BLOs swamps any intrinsic optical line features that might be present, leaving EUV and X-ray spectroscopy as the main tools for probing the photoionized gas near the central engine.

2. OBSERVATIONS AND DATA REDUCTION

Our spectroscopic measurements were carried out during two observing runs: 1993 June 16–20 and 1993 July 5–11 (total exposure times 132,836 s and 157,209 s, respectively). Whereas the July data were very clean and could all be used in the analysis, the June data were contaminated by atmospheric noise (e.g., Lieu et al. 1993). To delete the noisy data, we first plotted the time sequence and removed the most clearly identifiable spurious points by hand. We then determined the median and standard deviation of the remaining set and eliminated all data points that deviated by more than 2 σ from the median. This left 110,640 s of useful exposure time for the June observation.

Background subtraction was carried out by utilizing data from the sides of the spectrum in the two-dimensional detector image. We have considered N background strips, each having the same width as the spectrum, and binned the data in the dispersion direction in cells of size 0.5 Å (roughly the resolution element). Assuming Poisson statistics, the mean background at wavelength λ is $\bar{B}(\lambda) = \sum_{i=1}^{N} B_i(\lambda)/N$, where $B_i(\lambda)$ is the number of counts in the cell centered on λ in strip i, and the count number $S(\lambda)$ of the background-subtracted spectrum has a standard deviation $\sigma_S(\lambda) = [S(\lambda) + \bar{B}(\lambda)(1 + 1/N)]^{1/2}$. [The analogous expression for $\sigma_S(\lambda)$ in Fruscione et al. 1994 contains a typographical error.] Although the spectrometer size is such that four strips can be identified on each side of the spectrum, we have included only the central four strips in calculating the background because instrumental effects cause the background to be overestimated in the outer strips for $\lambda < 75$ Å. Figure 1 shows the resulting spectra obtained by dividing the background-subtracted counts by the effective area of the spectrometer (derived from in-orbit calibration measurements; Boyd et al. 1994) and by the useful observing time. Note that the spectral regime $\lambda < 75$ Å, where the background is both relatively high and uncertain, is excluded from the subsequent analysis.

One striking aspect of the spectra displayed in Figure 1 is the apparent presence of several absorption features, which indicates that line opacity has an important effect on the spectrum. The most prominent features appear as residuals from a power-law fit to the data that we made by using the Galactic H I column density N_G(H I) = 1.36×10^{20} cm^{-2} derived from the observed 21 cm emission in the direction of PKS 2155−304 (Albert et al. 1993). The best-fit spectral index is sensitive to the assumed He I/H I and He II/H I ratios: for values of 0.1 and 0.01, respectively (see Fruscione et al. 1994), $\alpha = 4.0 \pm 0.3$ for the June data and 4.3 ± 0.2 for the July data,

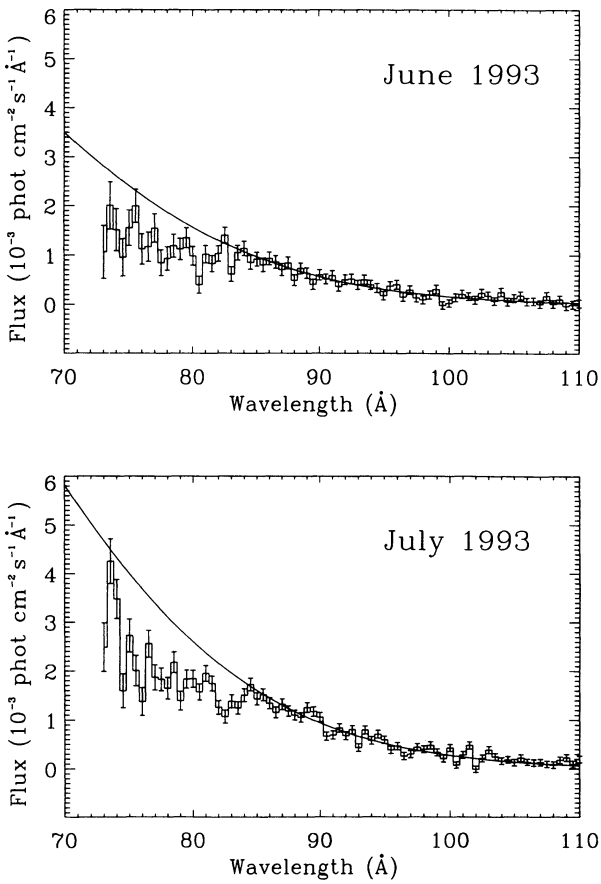

FIG. 1.—Background-subtracted spectrum (shown with 1 σ error bars) for the 1993 June (*top*) and July (*bottom*) *EUVE* observations of PKS 2155−304. The solid line in each case represents a best-fit (in the range 85–110 Å) α = 1.65 power-law continuum with Galactic absorption characterized by N_G(H I) = 1.36×10^{20} cm^{-2}, He I/H I = 0.1, and He II/H I = 0.01.

whereas for He I/H I = 0.07 and He II/H I = 0.023 (the values derived by Vennes et al. 1993 in the direction of GD 246), the corresponding indices are $\alpha = 2.5 \pm 0.3$ for June and 2.8 ± 0.2 for July. The number of ≥ 3 σ absorption features between 75 and 110 Å that one infers from these fits is two in June and five in July.

The total measured flux in the 75–110 Å range was $4.6 \pm 1.0 \times 10^{-12}$ ergs cm^{-2} s^{-1} during the first observation and $7.4 \pm 0.9 \times 10^{-12}$ ergs cm^{-2} s^{-1} during the second. For comparison, the flux measured by Fruscione et al. (1994) over the same wavelength interval was $2.3 \pm 1.0 \times 10^{-12}$ ergs cm^{-2} s^{-1} during the 1992 July calibration observation. Evidently, the spectrum varies on timescales of weeks and months in both shape and flux level.

3. INTERPRETATION

The spectral indices ($\alpha \gtrsim 3$) of the best power-law fits to the *EUVE* data are much steeper than the values measured in both the soft X-ray and the UV regimes, which suggests that the EUV spectrum cannot be represented by a simple power law. Based on the discussion in § 1, a plausible guess for the actual spectral index is the *ROSAT* PSPC value $\alpha \approx 1.65$. Fitting such a power-law continuum to the data implies strong absorption in the ~75–85 Å range, particularly for the July observation (see Fig. 1). To test whether this apparent flux

deficit could be attributed to *continuum* absorption at the source, we have employed the XSTAR photoionization code (kindly provided to us by T. Kallman) and calculated the expected spectra for different values of the ionization parameter $\xi \equiv L_{\rm ion}/n_{\rm H} r^2$ (where $n_{\rm H}$ is the hydrogen density, r is the distance to the continuum source, and $L_{\rm ion}$ is the ionizing luminosity [estimated to be $\sim 10^{46}\ h^{-2}$ ergs s^{-1} using the measured EUV flux, $z = 0.116$, and a Hubble constant $H_0 = 100\ h$ km s^{-1} Mpc^{-1}]). We found that strong continuum absorption at these wavelengths requires a total column density $N_{\rm tot} \gtrsim 5 \times 10^{20}$ cm^{-2} and occurs only for $\xi \lesssim 0.5$, but that, in that case, an even larger continuum opacity at longer wavelengths and very strong line-absorption features are predicted, both of which are inconsistent with the data.[4]

An alternative interpretation of the EUV data is that the observed spectrum arises in large part from a superposition of Doppler-smeared absorption lines that originate in a high-velocity, clumped outflow from the nucleus of PKS 2155−304. We have tested this scenario using the XSTAR code in conjunction with the hydromagnetic disk-driven wind model discussed in Königl & Kartje (1994). We have found that the gross features of the spectrum can be adequately reproduced by an outflow spanning a narrow range of ionization parameters and velocities around $\xi \gtrsim 10$ and $v \lesssim 0.1c$, respectively. Figure 2 presents an example of such a model fit, which demonstrates that both the overall ∼75–85 Å flux deficit and the appearance of distinct absorption features can be accounted for with this scenario. The dominant contributors to this moderate-ξ spectrum are L-shell transitions of intermediate-Z elements (notably Mg and Ne) as well as M-shell transitions of Fe.

For outflows observed at small (∼5°) angles to the symmetry axis, the hydromagnetic wind models considered by Königl & Kartje (1994) indicate that a velocity $\sim 0.1c$ is typically attained on a scale $r \approx 5 \times 10^{17} (M/10^8\ M_\odot)$ cm (where M is the mass of the central object). Using this length scale in the expression for the ionization parameter and adopting $\xi \approx 15$ and $L_{\rm ion} \approx 10^{46}$ ergs s^{-1} yield a density $n_{\rm H} \approx 3 \times 10^9$ cm^{-3} for the absorbing gas. The inferred values of r and n are characteristic of BELR clouds (see, e.g., Netzer 1990). By rescaling our continuous wind model to represent a clumped outflow (which we have done by assuming the invariance of ξ and $N_{\rm tot}$; see Krolik et al. 1985), we have deduced a cloud volume filling factor $f_V \approx 10^{-6} f_A (r/5 \times 10^{17}\ {\rm cm})^{-1}$ (where $f_A \lesssim 1$ is the cloud covering factor). Although it is conceivable that the clouds are entrained by the relativistic jet that propagates along the symmetry axis, their inferred subrelativistic speeds suggest that they are not located in the jet. The clouds must, however, cross our line of sight within the beamed emission cone of the relativistic outflow if they are to give rise to the observed absorption. One possibility is that the clouds are accelerated by a hydromagnetically driven wind that originates in the nuclear accretion disk, as in the BELR cloud model of Emmering, Blandford, & Shlosman (1992). However, the inferred value of $N_{\rm tot}$ ($\sim 5 \times 10^{20}$ cm^{-2}), which is a factor $\gtrsim 10^2$ lower than that of a standard BELR cloud, indicates that the clouds in this object are much smaller than typical BELR clouds in QSOs. This is consistent with the apparent dearth of BELR gas in PKS 2155−304 and in BLOs in general (e.g., Guilbert, Fabian, & McCray 1983), as well as with the order-of-magnitude higher velocities that we have deduced for the BLO clouds (since smaller clouds would be accelerated more efficiently).

[4] Potentially observable, but hitherto undetected, X-ray features are another problematic prediction of this interpretation.

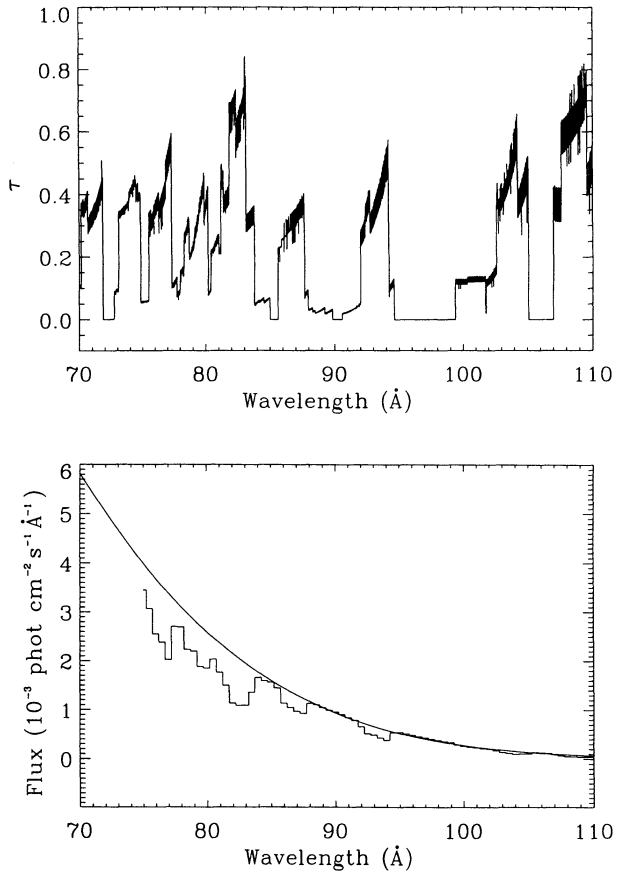

FIG. 2.—Model fit to the *EUVE* data for PKS 2155−304. The model represents a clumped outflow of total column density $N_{\rm tot} = 4.8 \times 10^{20}$ cm^{-2} that extends between $r_{\rm in}$ and $r_{\rm out} = 1.5 r_{\rm in}$, with $n_{\rm H} \propto r^{-1}$, $v \propto r^{-1}$, $v(r_{\rm min}) = 2 \times 10^9$ cm s^{-1}, and $\xi(r_{\rm min}) = 15$. The top panel presents the EUV line opacities, calculated by assuming cosmic abundance for all the elements and a source redshift of 0.116. The bottom panel shows the fit to the 1993 July data, normalized by minimizing the χ^2 statistic. The model spectrum was calculated by incorporating the effect of the outflow line and continuum opacity on an $\alpha = 1.65$ power-law continuum (represented by the solid curve) and using the Galactic absorption parameters listed in the legend to Fig. 1. The reduced χ^2 of this fit over the range 75–110 Å is 4.7 (71 d.o.f.), declining to 3.9 if the Galactic column is characterized instead by He I/H I = 0.07 and He II/H I = 0.023. The corresponding fit of this model to the 1993 June data has $\chi^2_{\rm red} = 2.7$ and 2.6, respectively, for these two sets of Galactic parameters.

Figure 3 exhibits the X-ray line opacity predicted by the clumped outflow model that was used to derive the EUV spectrum in Figure 2. The X-ray line spectrum is dominated by an O VII Kα feature that is broadened and blueshifted (relative to the cosmologically redshifted rest energy) by the motion of the absorbing gas. The overall shape of this feature appears to correspond roughly to that of the absorption feature detected in 1990 December by BBXRT (Madejski et al. 1994; see § 1). The maximum optical depth of the model feature is about an order of magnitude greater than that measured by BBXRT, although in making the comparison one should bear in mind that the BBXRT and the *EUVE* observations were not simultaneous. For a given combination of $N_{\rm tot}$ and of the Mg, Ne, and Fe abundances that reproduces the EUV data, the predicted optical depth of the X-ray feature can be adjusted by

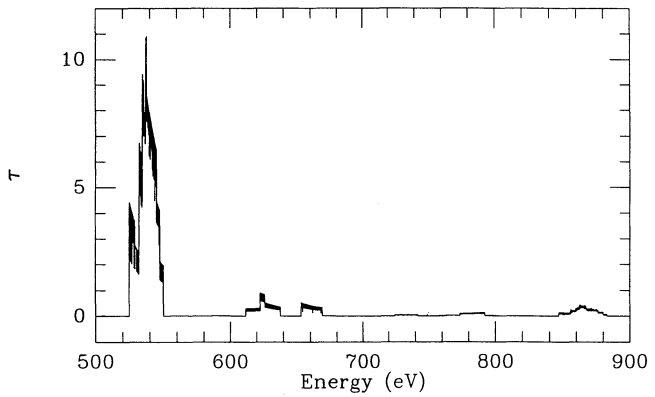

FIG. 3.—The predicted X-ray line opacities for the outflow model described in the legend to Fig. 2.

varying the relative abundance of oxygen (which, for $\xi \gtrsim 10$, does not affect the EUV spectrum below ~ 110 Å). We have verified that the alternative interpretation of the BBXRT observations in terms of an oxygen K-edge at a redshift in the range 0.18–0.42 (Madejski et al. 1994) is inconsistent with the *EUVE* observations, basically because of the large values of $N_{\rm tot}$ ($\gtrsim 5 \times 10^{21}$ cm^{-2}) that it involves. The EUV and X-ray data together thus reinforce the identification of this BLO with a galaxy at $z = 0.116$.

Our model of the EUV and X-ray spectra suggests that the absorbing gas is composed of high-velocity clouds that occupy a relatively narrow range of distances from the central object. Such a distribution could be associated with a nonsteady ejection episode that led to clouds with possibly different ξ and v distributions crossing our line of sight to the beamed continuum source at different times. This interpretation is consistent with the EUV spectral variability indicated by our observations (see Fig. 1) and also offers a possible explanation of the apparent X-ray spectral variability discussed in § 1. In particular, the *Einstein* OGS data could in principle be reconciled with the BBXRT observations if they represented a separate outflow component characterized by a higher value of ξ (due, e.g., to the absorbing clouds crossing our line of sight closer to the continuum source). For $\xi \gtrsim 10^2$, the abundance of O VIII would exceed that of O VII, and the X-ray absorption could be dominated by a Doppler-smeared O VIII Lyα line (see Königl & Kartje 1994, Figs. 11 and 12). Although these two inferred outflow components were observed a decade apart, they could be associated with a single outburst event: for example, they might be related to a disk instability wherein a propagating front induces an outflow at progressively larger radii (a situation that may resemble FU Orionis outbursts in pre–main-sequence stars; see, e.g., Calvet, Hartmann, & Kenyon 1993 and Bell & Lin 1994). Coordinated future EUV and X-ray observations could test whether the long-term X-ray spectral variability is correlated with changes in the EUV spectrum, as would be predicted by this picture, and whether such variations indeed exhibit a systematic trend in the underlying ionization and velocity structures.

We thank C. Dermer, A. Fruscione, T. Kallman, D. Liedahl, and M. Rees for valuable conversations. This work was supported in part by NASA grants NAG 5-2265 and NAGW-1636.

REFERENCES

Albert, C. E., Blades, J. C., Morton, D. C., Lockman, F. J., Proulx, M., & Ferrarese, L. 1993, ApJS, 88, 81
Bell, K. R., & Lin, D. N. C. 1994, ApJ, 427, 987
Blandford, R. D., & Rees, M. J. 1978, in Pittsburgh Conference on BL Lac Objects, ed. A. M. Wolfe (Pittsburgh: Univ. of Pittsburgh Press), 328
Bowyer, S., Lieu, R., Lampton, M., Lewis, J., Wu, X., Drake, J. J., & Malina, R. F. 1994, ApJS, 93, 569
Boyd, W., Jelinsky, P., Finley, D. S., Dupuis, J., Abbott, M., Christian, C., & Malina, R. F. 1994, in EUV, X-Ray, and Gamma-Ray Instrumentation for Astronomy V, ed. O. H. W. Siegmund & J. V. Vallerga (Proc. SPIE, 2280), in press
Brinkmann, W., et al. 1994, A&A, 288, 433
Calvet, N., Hartmann, L., & Kenyon, S. J. 1993, ApJ, 402, 623
Canizares, C. R., & Kruper, J. 1984, ApJ, 278, L99
Emmering, R. T., Blandford, R. D., & Shlosman, I. 1992, ApJ, 385, 460
Falomo, R., Pesce, J. E., & Treves, A. 1993, ApJ, 411, L63
Fruscione, A., Bowyer, S., Königl, A., & Kahn, S. M. 1994, ApJ, 422, L55
Guilbert, P. W., Fabian, A. C., & McCray, R. 1983, ApJ, 266, 466
Königl, A., & Kartje, J. F. 1994, ApJ, 434, 446
Krolik, J. H., Kallman, T. R., Fabian, A. C., & Rees, M. J. 1985, ApJ, 295, 104
Lieu, R., Bowyer, S., Lampton, M., Jelinsky, P., & Edelstein, J. 1993, ApJ, 417, L41
Madejski, G. M., et al. 1994, preprint
Maraschi, L., Maccacaro, T., & Ulrich, M.-H. 1989, BL Lac Objects (Berlin: Springer)
Marshall, H. L., Carone, T. E., & Fruscione, A. 1993, ApJ, 414, L53
Netzer, H. 1990, in Active Galactic Nuclei, ed. T. J. L. Courvoisier & M. Mayor (Berlin: Springer), 57
Ostriker, J. P., & Vietri, M. 1990, Nature, 344, 45
Pounds, K. A., et al. 1993, MNRAS, 260, 77
Urry, C. M., et al. 1993, ApJ, 414, 614
Vennes, S., Dupuis, J., Rumph, T., Drake, J., Bowyer, S., Chayer, P., & Fontaine, G. 1993, ApJ, 410, L119